

Finite temperature electric field induced two-dimensional coherent nonlinear spectroscopy in a Kitaev magnet

Wolfram Brenig^{1,*} and Olesia Krupnitska^{1,2,†}

¹*Institute for Theoretical Physics, Technical University Braunschweig, D-38106 Braunschweig, Germany*

²*Institute for Condensed Matter Physics, National Academy of Sciences of Ukraine, Svientsitskii Street 1, 790 11, L'viv, Ukraine*

We study electric field induced two-dimensional coherent nonlinear optical spectroscopy (2DCS) in a Kitaev magnet at finite temperature. We show that 2DCS is susceptible to both types of fractional quasiparticles of this quantum spin-liquid, i.e., fermions and flux visons. Focusing on the second order response, we find a strong antidiagonal feature in the two-dimensional frequency plane, related to the galvanoelectric effect of the fractional fermions. Perpendicular to the antidiagonal, the width of this feature is set by quasiparticle relaxation rates beyond the bare Kitaev magnet, thereby providing access to single-particle characteristics within the multi-particle 2DCS continuum. While the structure of the 2DCS susceptibility stems from the fermionic quasiparticles and displays Fermi blocking versus temperature, the emergent bond randomness which arises due to thermally populated visons strongly modifies the fermionic spectrum. Therefore also the presence of gauge excitations is manifest in the 2DCS susceptibility as the temperature is increased beyond the flux proliferation crossover. Our results are consistent with and extend previous findings on second harmonic generation in Kitaev magnets.

I. INTRODUCTION

Two-dimensional (2D) coherent nonlinear optical spectroscopy (2DCS) [1–3] can be viewed as an analog of 2D nuclear magnetic resonance [4–6]. Similar to the latter, and by Fourier transforming the nonlinear response of a system which is driven by particular sequences of incident ultrashort laser pulses [1–3], spectral information can be obtained in more than one frequency dimension. In molecules, low-dimensional semiconductors, and nano-materials, this has lead to a wealth of information about structure, electronic and vibrational excitations, dynamics, relaxation, and dephasing [3, 7–10].

Recently 2DCS has come into focus also to analyze excitations in many-body phases of correlated electronic and magnetic solid-state systems, studying magnons [11], solitons [12], Majorana fermions and visons [13–15], spinons [16–23], fractons [24], marginal Fermi liquids [25], and three-particle correlations in Anderson and Hubbard models [26]. Several of these studies [12–22, 24] focus on magnets from the topical research field of quantum spin liquids (QSL) [27]. In these magnets, fractionalization induced nonlocal elementary excitations lead to ubiquitous continua which cannot be disentangled into their constituents in the spectra of conventional linear response probes. Here the ability of 2DCS to separate homogeneous and inhomogeneous broadening [3, 28] has been highlighted as a promising tool to deconvolute fractionalized continua [12].

The planar Kitaev magnet [29] is among the QSLs of great current interest [30, 31]. It is an Ising model on the honeycomb lattice with compass anisotropy of its exchange and allows for fractionalization of spins into mo-

ble Majorana matter and \mathbb{Z}_2 gauge flux excitations (visons). The latter are localized in the absence of external magnetic fields [29]. The flux-free state can be treated analytically [29], displaying gapless fermionic quasiparticles. All spin correlations are short ranged [32]. At nonzero magnetic field, the spectrum acquires a gap and a chiral edge mode [29]. Mott-Hubbard insulators with strong spin-orbit coupling [33], like α - RuCl_3 [34], may display low-energy magnetic properties close to that of the Kitaev model. However, non-Kitaev exchange interactions in α - RuCl_3 lead to zigzag antiferromagnetic order below 7.1K [35]. Suppressing this order by in-plane magnetic fields [36, 37] opens up a range of $H||a \sim 7..9\text{T}$ which may host a low-temperature QSL [38–42]. Excitation continua observed in several linear probes, both, direct, i.e., Raman [43–45], inelastic neutron [46–49], and resonant X-ray scattering [50], as well as indirect, i.e., phonon spectra [51–56], and ultrasound propagation [57], have been attributed to fractionalization.

Theoretical analysis of 2DCS spectra of Kitaev magnets [13–15] has focused solely on the direct coupling of the driving external *magnetic* field component of the laser light to the spin and on zero temperature. While several options for coupling to the *electric* field component exist in quantum magnets, e.g. [58–63], they remain unexplored for 2DCS in QSLs. Recently, two investigations [64, 65] have made a step into that direction, considering higher-harmonic generation (HHG) in Kitaev magnets based on the electric-field induced exchange-striction mechanism [61]. While HHG is also a nonlinear spectroscopy, it lacks the 2D frequency information of 2DCS. Since both studies [64, 65] find that fingerprints of fractional quasiparticles can be read off from HHG spectra and, moreover, finite temperature was shown to have a strong impact [65], it seems highly desirable to extend such analysis into the 2D frequency plane.

In turn, in this paper, we study electric field driven 2DCS in a Kitaev QSL including the effects of finite tem-

* w.brenig@tu-bs.de

† olesia.krupnitska@tu-braunschweig.de

perature and focusing on the leading order nonlinear contribution. Key findings include an anomalously singular antidiagonal response in the 2D frequency plane. Perpendicular to the antidiagonal line, one-particle life-times of the fractional fermions can be read off within a spectrum that otherwise resembles a continuum due to fractionalization. Moreover, we observe that visons also have a strong impact on the global structure of 2DCS, however, leaving the antidiagonal line-width untouched. The paper is organized as follows: In Sec. II we summarize the model. Sec. III details our evaluation of the 2DCS susceptibilities for homogeneous and random gauge states, in Sec. III A and III B, respectively. Results and discussions are presented in Secs. IV A - IV C. A summary is given in Sec. V. To avoid unnecessary replication, App. A lists some known technicalities for completeness.

II. THE MODEL

We consider the Kitaev spin-model on the two dimensional honeycomb lattice [29]

$$H_0 = \sum_{\mathbf{l}, \alpha} J_{\alpha} S_{\mathbf{l}}^{\alpha} S_{\mathbf{l}+\mathbf{r}_{\alpha}}^{\alpha}, \quad (1)$$

with Ising exchange $J_{\alpha=x,y,z}$, which we set isotropic, i.e. $J_{\alpha} = J$ as in Fig. 1. In the absence of additional exchange interactions or external magnetic fields, the sign of J is irrelevant. If not denoted explicitly, we use J as the unit of energy.

The light-matter interaction between the electric field E and the spin system can be of diverse nature [62]. The details of the 2DCS spectra will depend on that. To make progress, we follow [64] and use a dipole-coupling $-P \cdot E$, based on the exchange-striction mechanism induced by orbital polarization [61, 62]

$$P = \frac{\partial H_0}{\partial E} = g \sum_{\mathbf{l}} (S_{\mathbf{l}}^x S_{\mathbf{l}+\mathbf{r}_x}^x - S_{\mathbf{l}}^y S_{\mathbf{l}+\mathbf{r}_y}^y). \quad (2)$$

We use an electric field $\mathbf{E} = E \mathbf{e}_{\perp,z}$ perpendicular to the z -bonds. P is the effective polarization operator and g is the magnetoelectric coupling constant. Before proceeding, we explicitly caution that strictly speaking finite g requires broken inversion symmetry [61]. I.e., currently existing approximate Kitaev systems may realize neither Eq. (1) nor (2), even though indications of ferroelectricity have been reported for α -RuCl₃ [66] and Na₂Co₂TeO₆ [67]. Despite these remarks, combining Eq. (1) and (2) provides for a legitimate case study of electric field induced 2DCS on a QSL, which is what we focus on. For Mott-insulators it has been suggested that $|g/J| \sim O(0.1)\text{cm/MV}$ can be reached [64].

Nonlinear susceptibilities of the polarization P at order N of E involve thermal expectation values which are rank- $(N+1)$ tensors of P [68]. Since the equilibrium density matrix obeys the symmetries of the Kitaev model,

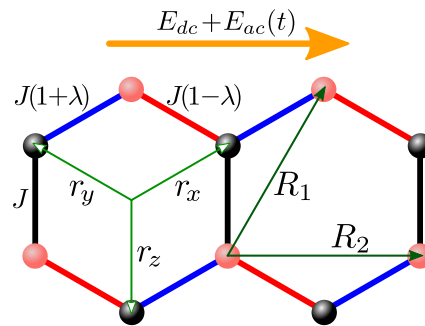


Figure 1. Kitaev model with (blue, red, black) x, y, z -bonds, hosting $S_{\mathbf{l}}^{\alpha} S_{\mathbf{l}+\mathbf{r}_{\alpha}}^{\alpha}$ exchange with $\alpha=x, y, z$, respectively. $\mathbf{l} = n_1 \mathbf{R}_1 + n_2 \mathbf{R}_2$ with basis vectors $\mathbf{R}_{1[2]} = (1, 0), [(\frac{1}{2}, \frac{\sqrt{3}}{2})]$ and $\mathbf{r}_{\alpha=x,y,z} = (\frac{1}{2}, \frac{1}{2\sqrt{3}}), (-\frac{1}{2}, \frac{1}{2\sqrt{3}}), (0, -\frac{1}{\sqrt{3}})$. In electric field $E_{dc} + E_{ac}(t) \perp$ to z -bonds, $J(1+\lambda, 1-\lambda, 1)$ refers to exchange interactions on x, y, z -bonds including dimerization $\lambda = -gE_{dc}$ by static field E_{dc} .

it is invariant under the operation U of simultaneous reflection on the z -bond $(x,y) \rightarrow (-x,y)$, including an exchange of spins $S^{x,y,z} \rightarrow (+, -, +)S^{y,x,z}$. The polarization and electric field both change sign under this operation. In turn, even- N susceptibilities vanish unless the U -symmetry of H_0 is broken.

Since $N = 2$ marks not only the lowest order nonlinear response, but also the leading order 2DCS susceptibility, it proves very useful that one can explicitly break the U -symmetry by retaining the *static*, i.e., DC component of the electric field. This approach is well known from field-induced second harmonic generation in semiconductors [69] or graphene [70] and it has been applied analogously for HHG generation in the Kitaev magnet [64, 65]. To see this, we decompose $E = E_{dc} + E_{ac}(t)$ into a static (DC) and a dynamic (AC) part, the latter of which time-averages to zero. As shown in Fig. 1, E_{dc} can be absorbed into a rescaled exchange $J_{\alpha} = J(1+\lambda, 1-\lambda, 1)$ with $\lambda = -gE_{dc}$. This dimerization breaks the U -symmetry.

Using the standard mapping to Majorana fermions and a static \mathbb{Z}_2 gauge field $\eta_{\mathbf{l}} = \pm 1$, residing on, e.g., the $\alpha = z$ bonds [29, 31], the Kitaev magnet with applied electric field reads

$$H_0 - P(E_{dc} + E_{ac}(t)) = H - PE_{ac}(t) = -\frac{i}{2} \sum_{\mathbf{l}, \alpha=x,y,z} J_{\alpha} \eta_{\mathbf{l}, \alpha} a_{\mathbf{l}} c_{\mathbf{l}+\mathbf{r}_{\alpha}} + \frac{i}{2} \sum_{\mathbf{l}, \alpha=x,y} \text{sg}_{\alpha} a_{\mathbf{l}} c_{\mathbf{l}+\mathbf{r}_{\alpha}} g E_{ac}(t), \quad (3)$$

where $\eta_{\mathbf{l}, x(y)} = 1, \eta_{\mathbf{l}, z} = \eta_{\mathbf{l}}$, and $\text{sg}_{\alpha} = +(-)$ for $\alpha = x(y)$. We choose to normalize the two Majorana fermions per unit cell according to $\{a_{\mathbf{l}}, a_{\mathbf{l}'}\} = \delta_{\mathbf{l}, \mathbf{l}'}, \{c_{\mathbf{l}}, c_{\mathbf{m}'}\} = \delta_{\mathbf{m}, \mathbf{m}'}$, and $\{a_{\mathbf{l}}, c_{\mathbf{m}}\} = 0$.

The expression (3) for the total Hamiltonian explicitly displays an additional reason for studying the optical exchange-striction coupling, namely, the Hamiltonian remains diagonal in the gauge flux, or speaking differently, this type of coupling to light does not excite visons. In

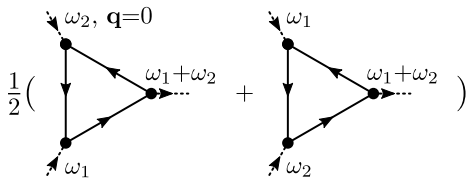


Figure 2. Diagrams for the 2DCS susceptibility $\chi_2(\omega_1, \omega_2)$ at order $O(2)$ in $E_{ac}(t)$. The solid lines carry a band index $\mu = 1, 2$, the dots refer to the 2×2 polarization operator matrices $p_{\mu\nu}$. I.e., the diagrams correspond to 2×8 expressions.

turn, visons will affect the 2DCS spectrum solely through their thermal occupation.

III. SECOND ORDER TWO-DIMENSIONAL RESPONSE FUNCTION

Technically, we are interested in the Fourier transform into the 2D frequency plane of the polarization response $\langle \Delta P \rangle(t)$ at $O(N=2)$ in $E_{ac}(t)$, i.e., the retarded susceptibility $\tilde{\chi}_2(t, t_1, t_2) = i^2 \Theta(t - t_1) \Theta(t_1 - t_2) \langle [P(t), P(t_1), P(t_2)] \rangle$ [65, 68]. This can be obtained from analytic continuation to the real axis of the Matsubara frequency transform of the fully connected contractions of the imaginary time propagator $\tilde{\chi}_2(\tau_2, \tau_1) = \langle T_\tau(P(\tau_2)P(\tau_1)P) \rangle$ [71, 72], i.e., the standard Feynman diagrams of Fig. 2. It should be noted that the N -fold time integrations in the perturbative expansion of the time-dependent density matrix at any order N in $PE_{ac}(t)$ are totally symmetric with respect to any permutation of the N time arguments, dubbed intrinsic permutation symmetry [68]. Therefore, any N -th order contributions to $\langle \Delta P \rangle(t)$ can be accounted for by the fully symmetrized susceptibility $\chi_N(t, t_1, \dots, t_n) = \sum_\pi \tilde{\chi}_N(t, t_{\pi(1)}, \dots, t_{\pi(N)})/N!$ [72], where π labels all permutations. This corresponds to the two diagrams of Fig. 2.

To evaluate Fig. 2, we consider two temperature regimes in this work, namely, above and below the flux proliferation temperature T^* . It is well established [31, 73–75] that in a narrow range of $0.01 \lesssim T/J \lesssim 0.05$ centered at T^* the \mathbb{Z}_2 flux gets thermally populated, rapidly changing the average gauge link density from $\langle \eta \rangle = 1$ to $\langle \eta \rangle = 0$. This allows to treat the Kitaev model at almost any temperature by considering a *homogeneous* flux state in Sec. III A for $T \lesssim T^*$ and a *random* flux state [76] for $T \gtrsim T^*$ in Sec. III B. This approach has proven to work well in studies of thermal conductivity [74, 75, 77], phonon renormalization [51, 52], and second harmonic generation [65], including almost quantitative agreement with exact diagonalization [74] and quantum Monte-Carlo [54, 55] where available. Finally, for the range of $0.01 \lesssim T/J \lesssim 0.05$, the impact of flux proliferation can be analyzed phenomenologically by considering a random flux state, however deliberately varying the average density of flipped links in the range of $[0, 1/2]$ while fixing the fermion temperature at $T \sim O(T^*)$.

A. Homogeneous flux state $T \lesssim T^*$

In the homogeneous flux ground-state, i.e., for $\eta_1 = 1$, Hamiltonian (1) can be diagonalized analytically in terms of complex Dirac fermions. Since this procedure is well documented, e.g., [31, 51, 52, 78] and many refs. therein, we merely quote the notations necessary to state our results. The Majorana fermions are mapped onto Dirac fermions on half of the momentum space by Fourier transforming $a(c)_{\mathbf{k}} = \sum_1 e^{-i\mathbf{k} \cdot \mathbf{1}} a(c)_1 / \sqrt{N}$ with momentum \mathbf{k} . They satisfy $a(c)_{\mathbf{k}}^\dagger = a(c)_{-\mathbf{k}}$. Fermionic anticommutation relations apply, $\{a_{\mathbf{k}}, a_{\mathbf{k}'}^\dagger\} = \delta_{\mathbf{k}, \mathbf{k}'}$, $\{c_{\mathbf{k}}, c_{\mathbf{k}'}^\dagger\} = \delta_{\mathbf{k}, \mathbf{k}'}$, and $\{a_{\mathbf{k}}^{(\dagger)}, c_{\mathbf{k}'}^{(\dagger)}\} = 0$. The diagonal form of H is

$$H = \sum_{\mathbf{k}, \gamma=1,2} \text{sg}_\gamma \epsilon_{\mathbf{k}} d_{\gamma\mathbf{k}}^\dagger d_{\gamma\mathbf{k}}, \quad (4)$$

where $[c_{\mathbf{k}}, a_{\mathbf{k}}]^T = \mathbf{u}(\mathbf{k}) [d_{1\mathbf{k}}, d_{2\mathbf{k}}]^T$ defines the quasiparticle fermions $d_{\gamma\mathbf{k}}$ via a unitary transformation $\mathbf{u}(\mathbf{k})$, listed in App. A, and $\text{sg}_\gamma = 1(-1)$ for $\gamma=1(2)$. The quasiparticles satisfy $d_{1(2)\mathbf{k}}^\dagger = d_{2(1)-\mathbf{k}}$, and \sum sums over half of momentum space. In Cartesian coordinates the quasiparticle energy $\epsilon_{\mathbf{k}}$ reads $\epsilon_{\mathbf{k}} = J[3 + 2\lambda^2 + 2(1 - \lambda^2) \cos(k_x) + 4 \cos(k_x/2) \cos(\sqrt{3}k_y/2) - 4\lambda \sin(k_x/2) \sin(\sqrt{3}k_y/2)]^{1/2}/2$. Similar to the Hamiltonian, the polarization can also be transformed into the diagonal Dirac fermion basis

$$P = g \sum_{\mathbf{k}, \mu\nu} d_{\mu\mathbf{k}}^\dagger p_{\mu\nu}(\mathbf{k}) d_{\nu\mathbf{k}}, \quad (5)$$

where, in Cartesian coordinates, $p_{11}(\mathbf{k}) = -p_{22}(\mathbf{k}) = \sin(k_x/2)(2\lambda \sin(k_x/2) - \sin(\sqrt{3}k_y/2))/(2\epsilon_{\mathbf{k}})$ and $p_{12}(\mathbf{k}) = p_{21}^*(\mathbf{k}) = -i \sin(k_x/2)(2 \cos(k_x/2) + \cos(\sqrt{3}k_y/2))/(2\epsilon_{\mathbf{k}})$. Evidently, P comprises inter- and intraband transitions.

Using Fig. 2, and Eqs. (4) and (5), it is now straightforward to evaluate the 2DCS susceptibility. We obtain

$$\chi_2(z_1, z_2) = g^3 \sum_{\mathbf{k}} \left[\frac{8(1-2f_{\mathbf{k}})\epsilon_{\mathbf{k}}^2 p_{11}(\mathbf{k})|p_{12}(\mathbf{k})|^2}{(z_1^2 - 4\epsilon_{\mathbf{k}}^2)(z_2^2 - 4\epsilon_{\mathbf{k}}^2)} \times \frac{(z_1^2 + z_1 z_2 + z_2^2 - 12\epsilon_{\mathbf{k}}^2)}{((z_1 + z_2)^2 - 4\epsilon_{\mathbf{k}}^2)} \right], \quad (6)$$

where $z_a = \omega_a + i\eta$ with $\eta \rightarrow 0^+$ and the Fermi function $f_{\mathbf{k}} = 1/(e^{\epsilon_{\mathbf{k}}/T} + 1)$.

B. Random flux state $T \gtrsim T^*$

For an arbitrary real-space distribution of $\{\eta_i\}$, the Majorana fermions on the $2N$ sites of the lattice are represented as a spinor $A_\sigma^\dagger = (a_1 \dots a_1 \dots a_N, c_1 \dots c_{1+\mathbf{r}_x} \dots c_N) := \mathbf{A}^\dagger$. Using the unitary Fourier-transform \mathbf{F} , constructed from two disjoint $N \times N$ blocks $F_{\sigma\rho}^{i=1,2} = e^{-i\mathbf{k}\sigma \cdot \mathbf{R}_\rho^i} / \sqrt{N}$, with $\sigma, \rho = 1 \dots N$ and $\mathbf{R}_\rho^i = \mathbf{1}$ and $\mathbf{1} + \mathbf{r}_x$, for a - and c -Majorana lattice sites, respectively, we map \mathbf{A} onto Dirac fermions by $\mathbf{D} = \mathbf{F}\mathbf{A}$. The

Brillouin zone is divided into pairs of $\pm\mathbf{k}$, with all $\mathbf{k} \neq -\mathbf{k}$ and in practice \mathbf{F} is rearranged such as to associate the $d_1^\dagger \dots d_N^\dagger$ with the $2(N/2) = N$ 'positive' \mathbf{k} -vectors. We then write

$$H = \mathbf{D}^\dagger \mathbf{h} \mathbf{D} / 2, \quad P = g \mathbf{D}^\dagger \mathbf{p} \mathbf{D} / 2, \quad (7)$$

for a given $\{\eta_l\}$, with \mathbf{h} and \mathbf{p} being $2N \times 2N$ matrices, in general nondiagonal and particle number nonconserving. Next, \mathbf{h} is diagonalized by a numerical Bogoliubov transformation \mathbf{U} onto quasiparticles $\mathbf{S} = \mathbf{U} \mathbf{D}$, for which $H = \sum_{\rho=1}^{2N} \epsilon_\rho S_\rho^\dagger S_\rho / 2$, with $(\mathbf{U} \mathbf{h} \mathbf{U}^\dagger)_{\rho\sigma} = \delta_{\rho\sigma} \epsilon_\rho$ and $\epsilon_\rho = (\epsilon_1 \dots \epsilon_N, -\epsilon_1 \dots -\epsilon_N)$. For the diagram calculations, we stay within the Nambu space of $\rho = 1 \dots 2N$, keeping the particle- and hole-range of $S_\rho^{(\dagger)}$.

The quasiparticle Green's function $G_{\alpha\beta}(\tau) = -\langle T_\tau (S_\alpha S_\beta^\dagger) \rangle$ in Matsubara frequency space reads $G_{\alpha\beta}(\varepsilon_n) = \delta_{\alpha\beta} / (i\varepsilon_n - \epsilon_\alpha)$ with $\varepsilon_n = (2n+1)\pi T$. It satisfies the following helpful identities $-\langle T_\tau (S_\alpha^\dagger S_\beta^\dagger) \rangle = -\langle T_\tau (S_\alpha S_\beta) \rangle = G_{\bar{\alpha}\bar{\beta}}(\tau)$ for the anomalous Green's functions, using the notation $\bar{\rho} = \rho \mp N$ for $\rho \geq N$. Equipped with this, and Fig. 2, and after some algebra we arrive at the 2DCS susceptibility

$$\chi_2(z_1, z_2) = g^3 \sum_{\alpha\beta\gamma} \frac{t_{\alpha\gamma} t_{\gamma\beta} t_{\beta\alpha}}{2(z_1 + z_2 - \epsilon_\alpha + \epsilon_\gamma)} \left[\begin{aligned} & (f_\alpha - f_\beta) \left(\frac{1}{z_2 - \epsilon_\alpha + \epsilon_\beta} + \frac{1}{z_1 - \epsilon_\alpha + \epsilon_\beta} \right) + \\ & (f_\gamma - f_\beta) \left(\frac{1}{z_2 - \epsilon_\beta + \epsilon_\gamma} + \frac{1}{z_1 - \epsilon_\beta + \epsilon_\gamma} \right) \end{aligned} \right], \quad (8)$$

for a fixed set of $\{\eta_l\}$, with Fermi function $f_\alpha = 1/(\exp(\epsilon_\alpha/T) + 1)$ and $t_{\alpha\beta} = (m_{\alpha\beta} - m_{\bar{\beta}\bar{\alpha}})/2$ from the Bogoliubov transform of the polarization $P = g \mathbf{S}^\dagger \mathbf{m} \mathbf{S} / 2$ which is not simultaneously diagonal with H , i.e., remains particle-number nonconserving. Finally and following ref. [74], \mathbf{U} , ϵ_α , $m_{\alpha\beta}$, and Eqs. (8) are calculated numerically for a sufficiently large number of random distributions $\{\eta_l\}$ and averaged over.

Eqs. (6) and (8) constitute the central formulas of this paper. Next, we discuss them from various perspectives.

IV. DISCUSSION

A. Preliminaries

We begin the discussion with some consistency checks of Eqs. (6) and (8). First, in the thermodynamic limit and for any general distribution $\{\eta_l\}$, there is no obvious algebraic relation between these two equations. However, one may consider the exemplary case of a single Bogoliubov-pair of states only in Eq. (8), with $\alpha = 1, 2$ and $\epsilon_{1,2} = \epsilon, -\epsilon$. Carrying out the sum on α, β, γ for that case, it is reassuring to realize that Eq. (8) then is identical to the contribution from a single \mathbf{k} -point in Eq. (6), identifying $\epsilon_{1,2} = \epsilon_{\mathbf{k}}, -\epsilon_{\mathbf{k}}$ and $t_{\alpha\beta} = p_{\alpha\beta}(\mathbf{k})$.

Next, setting $z_1 = z_2 = z$ the 2DCS susceptibilities describe the physics of second harmonic generation. This has been analyzed in ref. [65]. Therefore, we mention, that inserting this case into Eqs. (6) and (8), one indeed recovers Eqs. (7) and (12) of the above-mentioned work [65, 79].

Now, and for a more direct understanding of Eq. (6), we step back and motivate $\chi_2(z_1, z_2)$ at $T = 0$ by simple consideration of a two-level system. Since the homogeneous state is translationally invariant, and the wave vector of the laser light is practically zero, all excitations occur on a disjoint collection of pairs of states $\{\mathbf{1k}, 2\mathbf{k}\}$ with energies $\{\epsilon_{\mathbf{k}}, -\epsilon_{\mathbf{k}}\}$, enumerated by \mathbf{k} . In principle the levels in each two-level system refer to a Dirac fermion in either the upper or the lower band, however at $T = 0$ one may focus on a two-dimensional Hilbert space with a complete orthonormal set of eigenstates of the Hamiltonian $|1\rangle, \epsilon$ and $|2\rangle, -\epsilon$. I.e., $|1\rangle\langle 2|$ refers to the Dirac fermion being in the upper(lower) band. The Hamiltonian reads $H = \epsilon|1\rangle\langle 1| - \epsilon|2\rangle\langle 2|$ and in the interaction picture the 2×2 polarization operator is assumed to be $P = n|1\rangle\langle 1| - n|2\rangle\langle 2| + m e^{2i\epsilon t} |1\rangle\langle 2| + m^* e^{-2i\epsilon t} |2\rangle\langle 1|$. Note that P is consistent with Eq. (5) regarding the sign structure of the diagonal elements. For $\tilde{\chi}_2(t, t_1, t_2)$ at $T = 0$, the matrix element $c(t, t_1, t_2) = i^2 \langle 2| [[P(t), P(t_1)], P(t_2)] |2\rangle$ needs to be considered [80]

$$c(t, t_1, t_2) = 4n|m|^2 (\cos(2\epsilon(t_2 - t_1)) - \cos(2\epsilon(t_2 - t))). \quad (9)$$

Next, we allow for two driving frequencies of the electric field $E(t)$, i.e., $e^{-iz_1 t}$ and $e^{-iz_2 t}$ with $z_a = \omega_a + i\eta$, $\eta \rightarrow 0^+$, and perform the time ordered, elementary integrals over $c(t, t_1, t_2)$ to obtain the response $\langle \Delta P \rangle(t)$ as, e.g., in [65, 68, 72]. Finally we symmetrize over the permutations of z_1, z_2 as in Fig. 2, and get

$$\chi_2(z_1, z_2) = \frac{8\epsilon^2 n |m|^2 (z_1^2 + z_1 z_2 + z_2^2 - 12\epsilon^2)}{(z_1^2 - 4\epsilon^2)(z_2^2 - 4\epsilon^2)((z_1 + z_2)^2 - 4\epsilon^2)}. \quad (10)$$

Satisfyingly, this is identical to Eq. (6) except for reintroducing \mathbf{k} , the occupational prefactor $(1 - 2f_{\mathbf{k}})$, the replacement $n|m|^2 \rightarrow g^3 p_{11}(\mathbf{k}) p_{12}(\mathbf{k})^2$, and finally integrating over \mathbf{k} .

Anticipating the latter integration over \mathbf{k} and leaving the polarization matrix elements aside, we now analyze the contributions to Eq. (6) arising from the pole structures of Eq. (10). They comprise two kinds of singularities. The first kind occurs if only one of the differences of squares in the denominator vanishes. In the real $\omega_{1,2}$ -plane this produces simple δ -functions. Integrating them over $\epsilon \rightarrow \epsilon_{\mathbf{k}}$ as in Eq. (6) leads to finite and smooth contributions in the thermodynamic limit. The second kind of singularity occurs if two of the differences of squares in the denominator vanish simultaneously. This comprises four types of poles: (i) $z_1 = z_2 = \pm 2\epsilon$, (ii) $z_1 = -z_2 = \pm 2\epsilon$, (iii) $z_{1(2)} = \pm 2\epsilon$, $z_{2(1)} = 0$, and (iv) $z_{1(2)} = -z_{2(1)}/2 = \pm 2\epsilon$. Note that the singularity of type (i) marks a resonance of $\langle \Delta P \rangle(t)$ while keeping an output frequency $\omega_1 + \omega_2 = 2\omega_1$ which is twice the input. I.e., this is a resonant *second harmonic generation*

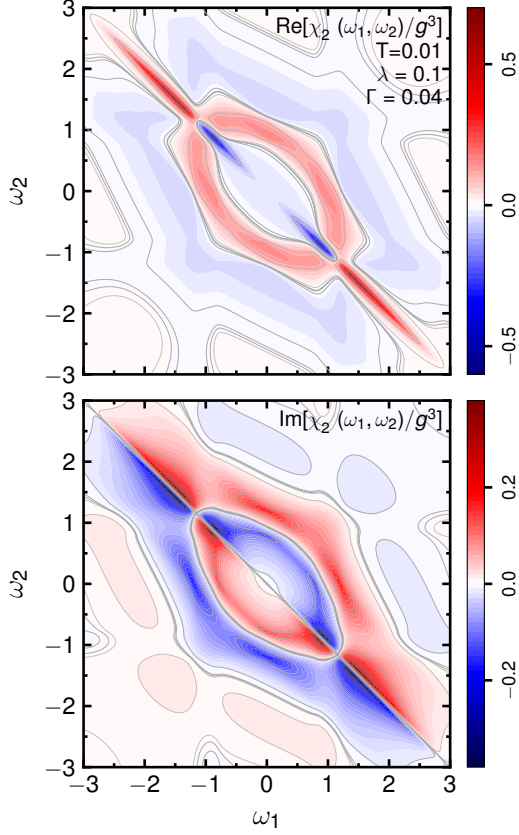


Figure 3. Contours of the real and imaginary part of the 2DCS susceptibility $\chi_2(\omega_1, \omega_2)$ in the homogeneous gauge state at fixed static field $\lambda = -gE_{dc}$. Linear system size $L=400$, energies in units of J .

(SHG). Similarly, type (ii) corresponds to a resonant response while keeping a DC output frequency $\omega_1 + \omega_2 = 0$. I.e., a resonant *galvanoelectric effect* (GEE). The asymptotic behavior of $\chi_2(z_1, z_2)/(n|m|^2)$ at one exemplary pole for each of the types, (i)-(iv), is

$$\begin{aligned}
 \text{(i)} \quad & \omega \equiv \omega_1 = \omega_2 \approx 2\epsilon, & \frac{1}{2\epsilon} \frac{1}{\omega - 2\epsilon + i\eta} \\
 \text{(ii)} \quad & \omega \equiv \omega_1 = -\omega_2 \approx 2\epsilon, & \frac{1}{2i\eta} \left(\frac{1}{\omega - 2\epsilon - i\eta} - \frac{1}{\omega - 2\epsilon + i\eta} \right) \\
 \text{(iii)} \quad & \omega \equiv \omega_1 \approx 2\epsilon, \quad \omega_2 = 0, & \frac{1}{i\eta} \left(\frac{1}{\omega - 2\epsilon + i\eta} - \frac{1}{\omega - 2\epsilon + 2i\eta} \right) \\
 \text{(iv)} \quad & \omega \equiv \omega_1 = -\frac{\omega_2}{2} \approx 2\epsilon, & \frac{1}{12\epsilon} \left(\frac{1}{\omega - 2\epsilon + i\eta} - \frac{1}{\omega - 2\epsilon - 2i\eta} \right)
 \end{aligned} \quad (11)$$

Integrating expressions of type (i), (iii), or (iv) over $\epsilon \rightarrow \epsilon_{\mathbf{k}}$ yields finite and smooth contributions to Eq. (6) in the thermodynamic limit. For type (iii) this stems from the term in the ()-brackets contributing only at $O(\eta)$. This leaves the type (ii) resonance on the GEE line. Asymptotically, for $\eta \ll 2\epsilon$, it can also be written as

$$\chi_2(z_1, z_2) = n|m|^2 \frac{\pi}{\eta} \delta(\omega_1 - 2\epsilon), \quad \omega_1 = -\omega_2 \approx 2\epsilon. \quad (12)$$

In turn, remarkably, $\chi_2(z_1, z_2)$ on the GEE line is anomalously singular, apart from being strictly real. I.e., integration of Eq. (12) over ϵ , as in Eq. (6), yields a response

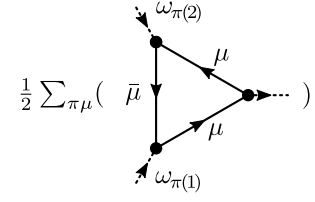


Figure 4. Diagrams contributing singularly to the GEE. π refers to the two permutations of input frequencies. $\mu=1,2$ refers to band index and $\bar{1}, \bar{2} = 2, 1$.

diverging $\propto 1/\eta$ as the causal broadening approaches zero [81]. Similar conclusions have also been drawn for the GEE in other contexts [71, 82–85]. Hereafter, and in order to regularize this singularity, we follow the latter works and replace the causal broadening η by a *physical relaxation rate* Γ which remains a free parameter. Since the Kitaev magnet maps to free Dirac fermions, we assume that Γ arises from many-body interactions beyond this model.

B. Homogeneous flux state $T \lesssim T^*$

To substantiate the preceding subsection, we now discuss several plots of $\chi_2(z_1, z_2)$. For that purpose we refrain from repeated explicit display of the broadening within the arguments of χ_2 , i.e., we set $\chi(\omega_1, \omega_2) \equiv \chi_2(\omega_1 + i\Gamma, \omega_2 + i\Gamma)$. In the homogeneous gauge state, the sole temperature dependence of the 2DCS susceptibility is due to the Fermi function in Eq. (6). For $T \ll J$ this is negligible. For numerical reasons we therefore fix $T = 0.01J \lesssim T^*$ in this subsection. In Fig. 3 contours of the 2DCS susceptibility are shown for a typical set of parameters, λ and Γ . This plot clearly features a main point of this work, associated with the analytic properties discussed using the two-level model. Namely, $\chi(\omega_1, \omega_2)$ is a smoothly varying function, except for a dominant anti-diagonal feature running along $\omega_2 = -\omega_1$. This feature is related exactly to the $1/\Gamma$ -singular contribution which stems from Eq. (12). As anticipated from that equation, the plot also shows that $\chi_2(\omega_1, -\omega_1)$ is purely real, with

$$\begin{aligned}
 \chi_2(\omega_1, -\omega_1) \simeq & \frac{\pi g^3}{\Gamma} \sum_{\mathbf{k}} [(1 - 2f_{\mathbf{k}}) p_{11}(\mathbf{k}) \times \\
 & |p_{12}(\mathbf{k})|^2 (\delta(\omega + 2\epsilon_{\mathbf{k}}) + \delta(\omega - 2\epsilon_{\mathbf{k}}))] . \quad (13)
 \end{aligned}$$

for $\Gamma \ll J$. At this point it is obvious that the identification of the causal broadening with a physical relaxation rate Γ can be generalized readily to include momentum dependence by replacing Γ with $\Gamma_{\mathbf{k}}$, moved into the summation over \mathbf{k} .

While Eq. (13) has already been made plausible via the two-level model, we also mention that it is straightforward to show that this singular behavior on the GEE line stems from 4 of the 16 graphs of Fig. 2, namely those depicted in Fig. 4. Moreover, and while the introduction

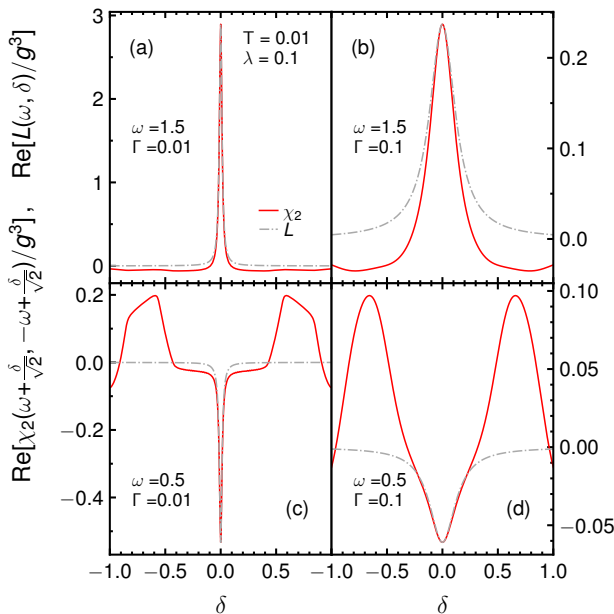


Figure 5. Real part of 2DCS susceptibility $\chi_2(\omega_1, \omega_2)$ in homogeneous gauge state, versus frequency δ perpendicular to the GEE line (solid red) at fixed static field $\lambda = -gE_{dc}$, compared to the asymptotic expression Eq. (14) (gray dashed dotted), for two exemplary frequencies on the GEE line ω and two exemplary relaxation rates Γ . Linear system size $L=400$, energies in units of J .

of Γ seems rather *ad-hoc*, it is also straightforward to show that introducing a phenomenological one-particle selfenergy, $\Sigma_{\mu, \mathbf{k}}(z) = i\Gamma_{\mu, \mathbf{k}} \text{sign}(\text{Im}(z))$, into the Dirac fermion Green's functions in Fig. 4 reproduces Eq. (13).

Next, we clarify the asymptotic behavior of $\chi_2(\omega_1, \omega_2)$ in the vicinity of the GEE line by introducing coordinates ω and δ , along and perpendicular to this line, $\omega_1 = \omega + \delta/\sqrt{2}$ and $\omega_2 = -\omega + \delta/\sqrt{2}$, respectively. Here, and from the discussion of Eq. (11) and for $\omega_1 \approx -\omega_2 \approx \pm 2\epsilon$, the poles of type $1/((\omega_1 + i\Gamma) \mp 2\epsilon_{\mathbf{k}})((\omega_2 + i\Gamma) \mp 2\epsilon_{\mathbf{k}})$ are relevant for $\omega_1 \geq 0$ in Eq. (6). Therefore, asymptotically

$$\begin{aligned} \chi_2(\omega_1, \omega_2) &\sim \int d\epsilon \rho(\epsilon, \omega_{1,2}) \frac{1}{\omega_1 + 2\epsilon + i\Gamma} \frac{1}{\omega_2 - 2\epsilon + i\Gamma} \\ &\sim \frac{i\sqrt{2}\Gamma \chi_2(\omega, -\omega)}{\delta + i\sqrt{2}\Gamma} \equiv L(\omega, \delta), \end{aligned} \quad (14)$$

where $\rho(\epsilon, \omega_{1,2})$ is a slowly varying function resulting from the non-singular contributions of the sum over \mathbf{k} in Eq. (6). To simplify, this is assumed to be constant performing the ϵ -integration. In Fig. 5 the asymptotic expression is compared with the actual 2DCS susceptibility for two selected frequencies ω . It shows reasonable agreement close to the GEE line.

The preceding clarifies another central point of this paper. Namely, tuning slightly off the GEE line, the real part of the 2DCS $O(2)$ low-frequency response displays a Lorentzian, the line width of which corresponds to the one-particle relaxation rate. I.e., 2DCS spectroscopy can

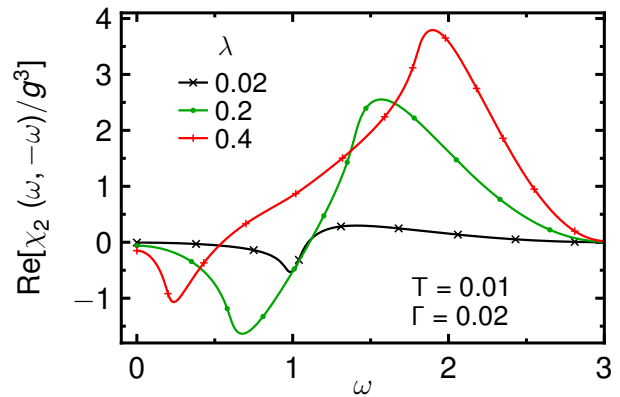


Figure 6. Real part of 2DCS susceptibility $\chi_2(\omega, -\omega)$ in homogeneous gauge state versus ω along the GEE line for various static fields $\lambda = -gE_{dc}$. Linear system size $L=400$, energies in units of J .

be used to disentangle the continuum of fermion excitations, generated by P , in order to access one-particle life-times.

Cutting through the contour plots of Fig. 3, two directions are of particular interest, i.e., $\omega_1 = \omega_2 = \omega$ and $\omega_1 = -\omega_2 = \omega$. The former refers to SHG and has been discussed in ref. [65]. The latter is the response function for the GEE. In Fig. 6 this is displayed for various DC fields. The figure also highlights the relevance of explicitly breaking the U -symmetry, discussed in Sec. II, in order to obtain a finite $O(2)$ 2DCS. I.e., for a vanishing DC field, $\lambda = 0$, the susceptibility vanishes and nonlinear response starts only at $O(3)$ of the electric field.

Finally, we mention that $\chi_2(z_1, z_2)$ shows a Fermi-blocking effect from the factor of $(1 - 2f_{\mathbf{k}})$ in Eq. (6). I.e., raising the temperature, the magnitude of the susceptibility decreases globally due to the blocking of occupied states. However, as mentioned already, within the temperature range $T \lesssim T^* \ll J$ of the homogeneous state, all temperature variations are very small only and we refrain from plotting this.

C. Random flux state $T \gtrsim T^*$

In this subsection we discuss 2DCS in a state with randomly flipped gauge links which models the thermal occupation of visons [51, 52, 65, 74, 75, 77]. We begin with an approximate description of the flux proliferation crossover of the 2DCS on the GEE line. While for $T > 0.05J$, flux in the Kitaev model is essentially random, freezing-out the vison excitations in the range of $0.01 \lesssim T/J \lesssim 0.05$ cannot be treated exactly for three-point correlation functions like $\chi_2(\omega_1, \omega_2)$ at present. Yet, a phenomenological understanding of the flux proliferation can be reached by fixing the fermion temperature at $T \sim 0.05$ and subsequently varying the average density of randomly flipped links $0 < n_\eta < 1/2$, thereby

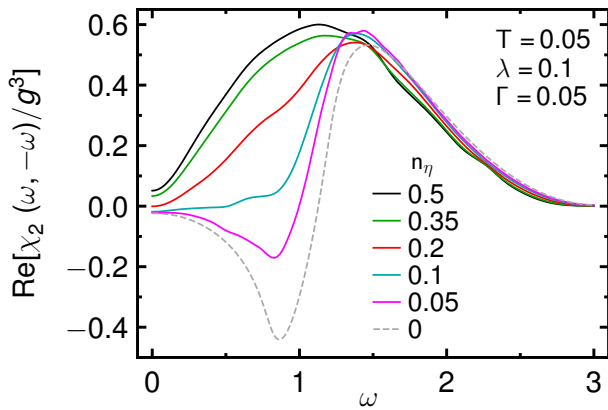


Figure 7. Solid colors: Real part of 2DCS susceptibility versus ω along the GEE line, for various flipped gauge link densities n_η at fixed temperature $T = 0.05$ and static field $\lambda = -gE_{dc}$. Linear system size $L = 30$, number of random realizations 62. Dashed: Same, however, in homogeneous gauge state with linear system size $L = 400$. Energies in units of J .

approximating the crossover between the homogeneous and the random gauge state. The effects of this are depicted in Fig. 7. First, the figure provides a satisfying consistency check, since $\chi_2(\omega, -\omega)$ obtained from the \mathbf{r} -space formalism encoded in Eq. (8) smoothly evolves into that from the \mathbf{k} -space formulation Eq. (6), as the density of flipped gauge links approaches zero. Second, the figure highlights another main point of this work, namely that vison excitations have a drastic impact on the susceptibility, suppressing an oscillatory behavior which is present without visons. In turn, not only the fingerprints of the fermionic fractional quasiparticles are encoded in the 2DCS response but also the second kind of fractional quasiparticles, i.e., visons impact the susceptibility.

Next we consider the vicinity of the GEE line in the presence of gauge excitations. As discussed in the previous subsection, in the homogeneous gauge state, the width of $\text{Re}[\chi_2(\omega_1, \omega_2)]$ allows to read off the one-particle relaxation rate Γ . Since gauge excitations leave the Kitaev model a two-band one-particle Hamiltonian, albeit with randomized energies and polarization operator matrix elements, no additional relaxation channel is introduced by visons. Therefore and as another main message, while on a global scale of the 2D frequency plane, visons will strongly modify the susceptibility, see Fig. 7, we expect the width of cuts perpendicular to GEE line, and in its vicinity, to remain insensitive to gauge excitations. Exactly this can be observed in Fig. 8. For two exemplary frequencies ω and damping rates Γ , the real part of the 2DCS susceptibility is not only shown in the homogeneous and the completely random gauge state, but for completeness also at flipped gauge link densities less than $1/2$. Obviously, visons do impact $\text{Re}[\chi_2(\omega_1, \omega_2)]$, even so far as to change its sign, similar to the low-frequency behavior in Fig. 7. However, the width of the central peak at $\delta \approx 0$ remains essentially unaffected. Therefore, it

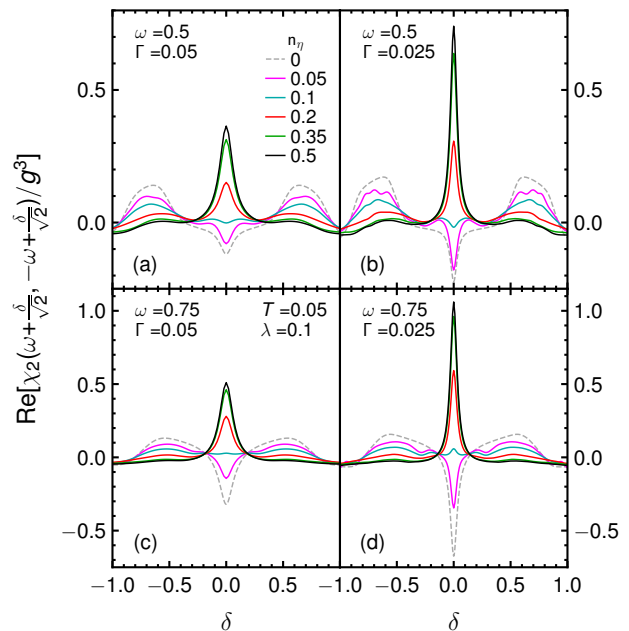


Figure 8. Real part of 2DCS susceptibility $\chi_2(\omega_1, \omega_2)$ versus frequency δ perpendicular to the GEE line (solid colors), for various flipped gauge link densities n_η , at fixed temperature $T = 0.05$ and static field $\lambda = -gE_{dc}$, compared to the asymptotic expression Eq. (14) (gray dashed), for two exemplary frequencies ω on the GEE line and for two exemplary damping rates Γ . Linear system size for randomized gauge $L=30$ with 62 random realizations, for homogeneous state $L=400$. Energies in units of J .

is tempting to speculate that any T -dependence of this GEE line-width may provide additional information on many-body interactions beyond the Kitaev model for all temperatures.

Finally, we show Fermi blocking in $\chi_2(\omega_1, \omega_2)$ for $T \gtrsim T^*$, i.e., in the fully random gauge state. This is displayed in Fig. 9 along the GEE line for $0.1J \leq T \leq J$. Clearly, the main feature of this plot is a continuous suppression of the 2DCS susceptibility upon increasing the temperature which results from fermionic states becoming blocked once they are thermally populated. This can be viewed as an evidence for the fermionic statistics of fractional excitations. It is completely in line with the same effect seen in SHG in ref. [65] and also reported for other spectroscopies in Kitaev magnets, including light scattering [43–45, 50], and phonon dynamics [51–57].

V. SUMMARY

In conclusion, we have studied electric field induced 2DCS in a Kitaev magnet at finite temperature. While the 2DCS susceptibility is set solely by the fermionic excitations and their coupling to the laser field, the fermionic spectrum is strongly modified by thermally excited visons. In turn, we find the 2DCS response to vary with temperature not only via Fermi statistics, but, far more

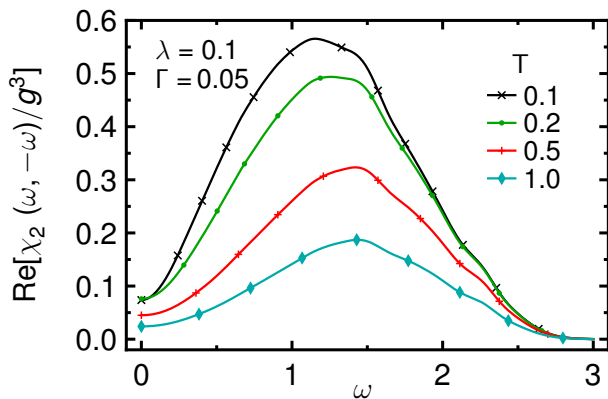


Figure 9. Real part of 2DCS susceptibility in random gauge state versus ω along the GEE line, for various temperatures T at fixed static field $\lambda = -gE_{dc}$. Linear system size $L = 30$, number of random realizations 62, energies in units of J .

importantly, also via intrinsic gauge randomness versus temperature. Strikingly, the 2DCS susceptibility displays a strong antidiagonal GEE singularity, which needs to be cut off by one-particle relaxation rates beyond the plain Kitaev model. These relaxation rates can be extracted from the 2DCS response perpendicular to the antidiagonal, which is robust against the gauge disorder at elevated temperatures. It is tempting to suggest that 2DCS experiments may therefore extract fractional quasiparticle lifetimes from a spectrum that is otherwise a featureless superposition of multi-particle excitations.

Our study has a number of loose ends that could be followed in future work. First, the combination of the Kitaev magnet and the coupling to electric fields via exchange-striction is motivated primarily by its simplicity. Other, more realistic couplings should be analyzed. It seems reasonable to speculate that gross features of the present work are robust, if more general dipole operators remain to mediate inter- and intraband transitions within the fermion bands. Second, the need for cutting off the singularity on the GEE line by a scattering rate, and apart from phenomenology, opens up a playground for interacting theories beyond the bare Kitaev model. This pertains to one-particle renormalizations, as well as to vertex corrections of the three-point 2DCS susceptibil-

ity. Interestingly, within a completely different context [26], such directions have been pursued for other models recently. Next, the present work has focused on the lowest order response, explicitly breaking symmetries via the DC field. Calculations should however also be performed for higher order response. Finally, electric field induced 2DCS should also be considered for quantum spin systems other than the Kitaev magnet.

ACKNOWLEDGMENTS

Fruitful discussions with R. Valentí, M. Möller, and D. Kaib are gratefully acknowledged. We thank A. Schwenke for critical reading of the manuscript. Research of W.B. was supported in part by the DFG through Project A02 of SFB 1143 (project-id 247310070) and by grant NSF PHY-2309135 to the Kavli Institute for Theoretical Physics (KITP). W.B. acknowledges kind hospitality of the PSM, Dresden.

Appendix A: Quasiparticles of homogeneous state

The unitary transformation $\mathbf{u}(\mathbf{k})$ to quasiparticles used in Sec. III A and detailed in several refs., e.g., [51] reads

$$\begin{bmatrix} c_{\mathbf{k}} \\ a_{\mathbf{k}} \end{bmatrix} = \begin{bmatrix} u_{11}(\mathbf{k}) & u_{12}(\mathbf{k}) \\ u_{21}(\mathbf{k}) & u_{22}(\mathbf{k}) \end{bmatrix} \begin{bmatrix} d_{1\mathbf{k}} \\ d_{2\mathbf{k}} \end{bmatrix} \quad (\text{A1})$$

$$u_{11}(\mathbf{k}) = -u_{12}(\mathbf{k}) = \frac{i \sum_{\alpha} e^{-i\mathbf{k}\cdot\mathbf{r}_{\alpha}}}{2^{3/2} \epsilon_{\mathbf{k}}}$$

$$u_{21}(\mathbf{k}) = u_{22}(\mathbf{k}) = \frac{1}{\sqrt{2}},$$

where $\mathbf{k} = x \mathbf{G}_1 + y \mathbf{G}_2$ with $x, y \in [0, 2\pi[$ and $\mathbf{G}_{1[2]} = (1, -\frac{1}{\sqrt{3}}) [(0, \frac{2}{\sqrt{3}})]$ is the reciprocal basis of the triangular lattice with the direct basis listed in Fig. 1. From this $\mathbf{u}(\mathbf{k})$, a quasiparticle energy of $\epsilon_{\mathbf{k}} = J[3 + 2\lambda^2 + 2(1 - \lambda^2) \cos(x) + 2(1 - \lambda) \cos(x - y) + 2(1 + \lambda) \cos(y)]^{1/2}/2$ is obtained in terms of the reciprocal coordinates, as well as the matrix elements of the dipole operator $p_{11}(\mathbf{k}) = -p_{22}(\mathbf{k}) = (\cos(y) - \cos(x - y) + 2\lambda(1 - \cos(x)))/(4\epsilon_{\mathbf{k}})$ and $p_{12}(\mathbf{k}) = p_{21}^*(\mathbf{k}) = -i(\sin(x - y) + 2\sin(x) + \sin(y))/(4\epsilon_{\mathbf{k}})$, also expressed in reciprocal coordinates.

[1] S. Mukamel, *Annu. Rev. Phys. Chem.* **51**, 691 (2000).
[2] T. Brixner, T. Mančal, I. V. Stiopkin, and G. R. Fleming, *J. Chem. Phys.* **121**, 4221 (2004).
[3] M. Cho, *Chem. Rev.* **108**, 1331 (2008).
[4] A. Bax and L. Lerner, *Science* **23**, 1986 (1986).
[5] R. R. Ernst, G. Bodenhausen, A. Wokaun, *Nuclear Magnetic Resonance in One and Two Dimensions*, Oxford University Press, Oxford (1987).
[6] J. Jeener, *The unpublished Basko Polje (1971) lecture notes about two-dimensional NMR spectroscopy* INIS

[7] N. Huse, B. D. Bruner, M. L. Cowan, J. Dreyer, E. T. J. Nibbering, R. J. D. Miller, and T. Elsaesser, *Phys. Rev. Lett.* **95**, 147402 (2005).
[8] M. L. Cowan, B. D. Bruner, N. Huse, J. R. Dwyer, B. Chugh, E. T. J. Nibbering, T. Elsaesser, and R. J. D. Miller, *Nature* **434**, 199 (2005).
[9] W. Kuehn, K. Reimann, M. Woerner, and T. Elsaesser, *The Journal of Chemical Physics* **130**, 164503 (2009).
[10] W. Kuehn, K. Reimann, M. Woerner, T. Elsaesser, and R. Hey, *J. Phys. Chem. B* **115**, 5448 (2011).

- [11] J. Lu, X. Li, H. Y. Hwang, B. K. Ofori-Okai, T. Kurihara, T. Suemoto, and K. A. Nelson, *Phys. Rev. Lett.* **118**, 207204 (2017).
- [12] Y. Wan and N. P. Armitage, *Phys. Rev. Lett.* **122**, 257401 (2019).
- [13] W. Choi, K. H. Lee, and Y. B. Kim, *Phys. Rev. Lett.* **124**, 117205 (2020).
- [14] M. K. Negahdari and A. Langari, *Phys. Rev. B* **107**, 134404 (2023).
- [15] Y. Qiang, V. L. Quito, T. V. Trevisan, and P. P. Orth, arXiv:2301.11243.
- [16] Z.-L. Li, M. Oshikawa, and Y. Wan, *Phys. Rev. X* **11**, 031035 (2021).
- [17] G. Sim, J. Knolle, and F. Pollmann, *Phys. Rev. B* **107**, L100404 (2023).
- [18] Q. Gao, Y. Liu, H. Liao, and Y. Wan, *Phys. Rev. B* **107**, 165121 (2023).
- [19] G. Sim, F. Pollmann, and J. Knolle, *Phys. Rev. B* **108**, 134423 (2023).
- [20] Z.-L. Li and Y. Wan, *Phys. Rev. B* **108**, 165151 (2023).
- [21] M. Potts, R. Moessner, and O. Benton, arXiv:2311.03200.
- [22] Y. Watanabe, S. Trebst, and C. Hickey, arXiv:2401.17266.
- [23] R. Valentí, M. Möller, and D. Kaib, *private communication*.
- [24] R. M. Nandkishore, W. Choi, and Y. B. Kim, *Phys. Rev. Research* **3**, 013254 (2021).
- [25] F. Mahmood, D. Chaudhuri, S. Gopalakrishnan, R. Nandkishore, and N. P. Armitage, *Nat. Phys.* **17**, 627 (2021).
- [26] P. Kappl, F. Krien, C. Watzenböck, and K. Held, *Phys. Rev. B* **107**, 205108 (2023).
- [27] L. Savary and L. Balents, *Rep. Prog. Phys.* **80**, 016502 (2016).
- [28] S. T. Cundiff and S. Mukamel, *Physics Today* **66**, **44** (2013).
- [29] A. Kitaev, *Annals of Physics* **321**, 2 (2006).
- [30] H. Takagi, T. Takayama, G. Jackeli, G. Khaliullin, and S. E. Nagler, *Nat Rev Phys* **1**, 264 (2019).
- [31] Y. Motome and J. Nasu, *J. Phys. Soc. Jpn.* **89**, 012002 (2019).
- [32] G. Baskaran, S. Mandal, and R. Shankar, *Phys. Rev. Lett.* **98**, 247201 (2007).
- [33] G. Jackeli and G. Khaliullin, *Phys. Rev. Lett.* **102**, 017205 (2009).
- [34] K. W. Plumb, J. P. Clancy, L. J. Sandilands, V. V. Shankar, Y. F. Hu, K. S. Burch, H.-Y. Kee, and Y.-J. Kim, *Phys. Rev. B* **90**, 041112 (2014).
- [35] H. B. Cao, A. Banerjee, J.-Q. Yan, C. A. Bridges, M. D. Lumsden, D. G. Mandrus, D. A. Tennant, B. C. Chakoumakos, and S. E. Nagler, *Phys. Rev. B* **93**, 134423 (2016).
- [36] J. A. Sears, Y. Zhao, Z. Xu, J. W. Lynn, and Y.-J. Kim, *Phys. Rev. B* **95**, 180411 (2017).
- [37] A. U. B. Wolter, L. T. Corredor, L. Janssen, K. Nenkov, S. Schönecker, S.-H. Do, K.-Y. Choi, R. Albrecht, J. Hunger, T. Doert, M. Vojta, and B. Büchner, *Phys. Rev. B* **96**, 041405 (2017).
- [38] S.-H. Baek, S.-H. Do, K.-Y. Choi, Y. S. Kwon, A. U. B. Wolter, S. Nishimoto, J. van den Brink, and B. Büchner, *Phys. Rev. Lett.* **119**, 037201 (2017).
- [39] R. Hentrich, A. U. B. Wolter, X. Zotos, W. Brenig, D. Nowak, A. Isaeva, T. Doert, A. Banerjee, P. Lampen-Kelley, D. G. Mandrus, S. E. Nagler, J. Sears, Y.-J. Kim, B. Büchner, and C. Hess, *Phys. Rev. Lett.* **120**, 117204 (2018).
- [40] C. Balz, P. Lampen-Kelley, A. Banerjee, J. Yan, Z. Lu, X. Hu, S. M. Yadav, Y. Takano, Y. Liu, D. A. Tennant, M. D. Lumsden, D. Mandrus, and S. E. Nagler, *Phys. Rev. B* **100**, 060405 (2019).
- [41] R. Schönemann, S. Imajo, F. Weickert, J. Yan, D. G. Mandrus, Y. Takano, E. L. Brosha, P. F. S. Rosa, S. E. Nagler, K. Kindo, and M. Jaime, *Phys. Rev. B* **102**, 214432 (2020).
- [42] C. Balz, L. Janssen, P. Lampen-Kelley, A. Banerjee, Y. H. Liu, J.-Q. Yan, D. G. Mandrus, M. Vojta, and S. E. Nagler, *Phys. Rev. B* **103**, 174417 (2021).
- [43] L. J. Sandilands, Y. Tian, K. W. Plumb, Y.-J. Kim, and K. S. Burch, *Phys. Rev. Lett.* **114**, 147201 (2015).
- [44] J. Nasu, J. Knolle, D. L. Kovrizhin, Y. Motome, and R. Moessner, *Nature Physics* **12**, 912 (2016).
- [45] D. Wulferding, Y. Choi, S.-H. Do, C. H. Lee, P. Lemmens, C. Faugeras, Y. Gallais, and K.-Y. Choi, *Nat Commun* **11**, 1 (2020).
- [46] J. Knolle, D. L. Kovrizhin, J. T. Chalker, and R. Moessner, *Phys. Rev. Lett.* **112**, 207203 (2014).
- [47] [1] A. Banerjee, C. A. Bridges, J.-Q. Yan, A. A. Aczel, L. Li, M. B. Stone, G. E. Granroth, M. D. Lumsden, Y. Yiu, J. Knolle, S. Bhattacharjee, D. L. Kovrizhin, R. Moessner, D. A. Tennant, D. G. Mandrus, and S. E. Nagler, *Nature Materials* **15**, 733 (2016).
- [48] A. Banerjee, J. Yan, J. Knolle, C. A. Bridges, M. B. Stone, M. D. Lumsden, D. G. Mandrus, D. A. Tennant, R. Moessner, and S. E. Nagler, *Science* **356**, 1055 (2017).
- [49] S.-H. Do, S.-Y. Park, J. Yoshitake, J. Nasu, Y. Motome, Y. S. Kwon, D. T. Adroja, D. J. Voneshen, K. Kim, T.-H. Jang, J.-H. Park, K.-Y. Choi, and S. Ji, *Nature Phys* **13**, 1079 (2017).
- [50] G. B. Halász, N. B. Perkins, and J. van den Brink, *Phys. Rev. Lett.* **117**, 127203 (2016).
- [51] A. Metavitsiadis and W. Brenig, *Phys. Rev. B* **101**, 035103 (2020).
- [52] A. Metavitsiadis, W. Natori, J. Knolle, and W. Brenig, *Phys. Rev. B* **105**, 165151 (2022).
- [53] M. Ye, R. M. Fernandes, and N. B. Perkins, *Phys. Rev. Research* **2**, 033180 (2020).
- [54] K. Feng, M. Ye, and N. B. Perkins, *Phys. Rev. B* **103**, 214416 (2021).
- [55] K. Feng, S. Swarup, and N. B. Perkins, *Phys. Rev. B* **105**, L121108 (2022).
- [56] H. Li, T. T. Zhang, A. Said, G. Fabbris, D. G. Mazzone, J. Q. Yan, D. Mandrus, G. B. Halász, S. Okamoto, S. Murakami, M. P. M. Dean, H. N. Lee, and H. Miao, *Nat Commun* **12**, 3513 (2021).
- [57] A. Hauspurg, S. Zherlitsyn, T. Helm, V. Felea, J. Wosnitza, V. Tsurkan, K.-Y. Choi, S.-H. Do, M. Ye, W. Brenig, and N. B. Perkins, arXiv:2303.09288.
- [58] J. Lorenzana and G. A. Sawatzky, *Phys. Rev. Lett.* **74**, 1867 (1995).
- [59] H. Katsura, N. Nagaosa, and A. V. Balatsky, *Phys. Rev. Lett.* **95**, 057205 (2005).
- [60] C. Jia, S. Onoda, N. Nagaosa, and J. H. Han, *Phys. Rev. B* **76**, 144424 (2007).
- [61] H. Katsura, M. Sato, T. Furuta, and N. Nagaosa, *Phys. Rev. Lett.* **103**, 177402 (2009).
- [62] Y. Tokura, S. Seki, and N. Nagaosa, *Rep. Prog. Phys.* **77**, 076501 (2014).

- [63] R. Chari, R. Moessner, and J. G. Rau, Phys. Rev. B **103**, 134444 (2021).
- [64] M. Kanega, T. N. Ikeda, and M. Sato, Phys. Rev. Research **3**, L032024 (2021).
- [65] O. Krupnitska and W. Brenig, Phys. Rev. B **108**, 075120 (2023).
- [66] X. Mi, D. Hou, X. Wang, C. Liu, Z. Xiong, H. Li, A. Wang, Y. Chai, Y. Qi, W. Li, X. Zhou, Y. Su, D. I. Khomskii, M. He, Z. Sheng, and Y. Sun, *arXiv:2205.09530*.
- [67] S. Mukherjee, G. Manna, P. Saha, S. Majumdar, and S. Giri, Phys. Rev. Materials **6**, 054407 (2022).
- [68] P. N. Butcher, D. Cotter, The Elements of Nonlinear Optics, Cambridge University Press, Cambridge, 1990.
- [69] O. A. Aktsipetrov, A. A. Fedyanin, E. D. Mishina, A. N. Rubtsov, C. W. van Hasselt, M. A. C. Devillers, and Th. Rasing, Phys. Rev. B **54**, 1825 (1996).
- [70] A. Y. Bykov, T. V. Murzina, M. G. Rybin, and E. D. Obraztsova, Phys. Rev. B **85**, 121413 (2012).
- [71] D. E. Parker, T. Morimoto, J. Orenstein, and J. E. Moore, Phys. Rev. B **99**, 045121 (2019).
- [72] H. Rostami, M. I. Katsnelson, G. Vignale, and M. Polini, Annals of Physics **431**, 168523 (2021).
- [73] J. Nasu, M. Udagawa, and Y. Motome, Phys. Rev. B **92**, 115122 (2015).
- [74] A. Metavitsiadis, A. Pidotella, and W. Brenig, Phys. Rev. B **96**, 205121 (2017).
- [75] A. Pidotella, A. Metavitsiadis, and W. Brenig Phys. Rev. B **99**, 075141 (2019).
- [76] The term “random flux state” is used to imply an average over Hilbert space sectors with fixed, random values of η .
- [77] A. Metavitsiadis and W. Brenig, Rev. B **96**, 041115(R) (2017).
- [78] A. Metavitsiadis and W. Brenig, Phys. Rev. B **104**, 104424 (2021).
- [79] In ref. [65] the susceptibilities $\chi_{N\omega}(\omega)$ are listed with a global sign of -1^{N-1} .
- [80] Up to the fermionic occupation prefactor of $(1 - 2f_{\mathbf{k}})$ and the replacement $n|m|^2 \rightarrow g^3 p_{11}(\mathbf{k})|p_{12}(\mathbf{k})|^2$. This is exactly Eq. (B2) of ref. [65], which was derived however using the equations of motion for the Dirac fermions.
- [81] Analysis of an exponentially ramped two-level Floquet Hamiltonian with a driving polarization as in this work, yields a resonant GEE, which at second order is fully consistent with Eq. (12)
- [82] J. E. Sipe and A. I. Shkrebtii, Phys. Rev. B **61**, 5337 (2000).
- [83] R. Fei, W. Song, and L. Yang, Phys. Rev. B **102**, 035440 (2020).
- [84] H. Ishizuka and M. Sato, Phys. Rev. Lett. **129**, 107201 (2022).
- [85] A. Raj, S. Chaudhary, and G. A. Fiete, Phys. Rev. Research **6**, 013048 (2024).